Slotted and Notched Rectangular Antenna Designed for Biomedical Applications

Antena Rectangular con Ranuras y Muescas para Aplicaciones Biomédicas

Pedro Vargas-Chable[1,2], Margarita Tecpoyotl-Torres[*,1], Ramon Cabello-Ruiz[2], and Jose Mireles Jr. Garcia[3]

[1]Instituto de Investigación en Ciencias Básicas y Aplicadas-Centro de Investigación en Ingeniería y Ciencias Aplicadas, (IICBA-CIICAp) de la Universidad Autónoma del Estado de Morelos (UAEM)
Av. Universidad No. 1001, Col. Chamilpa, 62209, Cuernavaca, Morelos, México
[2]Facultad de Ciencias Químicas e Ingeniería (FCQeI),Universidad Autónoma del Estado de Morelos (UAEM)
Av. Universidad No. 1001, Col. Chamilpa, 62209, Cuernavaca, Morelos, México
[3]Centro de Investigación en Ciencia y Tecnología Aplicada (CICTA), Universidad Autónoma de Ciudad Juárez (UACJ)
Av. Plutarco Elías Calles No. 1210, Fovissste Chamizal, 32310, Ciudad Juárez, México
*tecpoyotl@uaem.mx

KEYWORDS:

2.4 GHz, Bandwidth, Gain, Ansys Electronics, HFSS

ABSTRACT

This paper presents the design and simulation of a microstrip-fed patch antenna for biomedical applications using FR-4 as substrate. The optimization of its response is performed by parameterizing elements, starting from (1) a simple rectangular antenna, (2) an array of slots in the right side, (3) slots and cuts in the corners of the antenna, (4) with the elements of (3) and a top notch in the patch, obtaining an evolution until obtaining (5) an antenna in which all the parameterized elements are integrated. The variation of the rectangular antenna response starts from model (1) with f_r=2.22 GHz, G=2.22 dB, S11=-22.81, BW=118.8 MHz, at 2.24 GHz, VSWR=1.25 dB and efficiency of 0.085, to model (5) with f_r=2.5 GHz, VSWR=1.35 dB, G=2.96 dB, S11=-22.16 dB, BW=69 MHz at 2.54 GHz and efficiency of 0.47. That is, improving the relevant antenna parameters, gain by 34.54% and efficiency by 552.94%.

PALABRAS CLAVE:

2.4 GHz, Ancho de banda, Ganancia, Ansys Electronics, HFSS

RESUMEN

En este artículo se presenta el diseño y simulación de una antena de parche con alimentación por microtira para aplicaciones biomédicas utilizando como substrato FR-4. La optimización de su respuesta se realiza parametrizando elementos, a partir de (1) una antena rectangular sencilla, (2) un arreglo de ranuras en la parte lateral derecha, (3) ranuras y cortes en las esquinas de la antena, (4) con los elementos de (3) y una muesca superior en el parche, obteniendo una evolución hasta obtener a (5) una antena en la que se integran a todos los elementos parametrizados. La variación de la respuesta de la antena rectangular parte del modelo (1) con f_r=2.22 GHz, G=2.22 dB, S11=-22.81, BW=118.8 MHz, a 2.24 GHz, VSWR=1.25 dB y eficiencia de 0.085, al modelo (5) con f_r=2.5 GHz, VSWR=1.35 dB, G=2.96 dB, S11=-22.16 dB, BW=69 MHz a 2.54 GHz y eficiencia de 0.47. Esto es, mejorando los parámetros relevantes de la antena, a la ganancia en un 34.54% y la eficiencia en 552.94%.

• **Recibido: 23 de noviembre de 2023** • **Aceptado: 10 de febrero de 2024** • **Publicado en línea: 1 de junio de 2024**

1. INTRODUCTION

In recent years, patch antennas have had a great evolution, mainly for specific applications in biomedicine [1]-[3]. The versatility to configure them, the ease to implement different geometric designs that allow to obtain configurations at operating frequencies and punctual bandwidths, make it an excellent option to continue in the characterization of signals that respond to wavelengths friendly to the human body, for

DOI: 10.30973/progmat/2024.16.2/1

animals, in nature and in some little explored ecosystems [4], [5]. According to [1],[2] for the Medical Implant Communications Service (MICS) communications are carried out in bands ranging from 402 MHz to 405 MHz. On the other hand, in the industrial, medical, and scientific sectors, communications range from 2.4 GHz to 2.48 GHz [3].

Two strategies to optimize these resonator devices are the application of cuts in the corners of the geometry and the realization of perforations or slots [6]-[8], which are simple to implement by parameterization or geometric ratios that allow to improve the gain (G), the operation frequency (f_c or f_r), Standing Wave Ratio (VSWR), Reflection Coefficient (S11), efficiency and radiation patterns [9],[10], so that they can resonate at the given operating frequency, as well as within the reference relative permittivity and conductivity parameters for specific biomedical applications [1]-[3].

With the support of numerical methods and CAD software, accurate approximations can be obtained for implementation in the laboratory and in specific applications, so it is important to carry out a simulation to understand the functionality of the device. In this work, Ansys Electronics student version is used, which allows to calculate the fundamental parameters and to have a broad overview of the antenna operation.

The structure of this article is as follows: In Section 1, a brief introduction is presented. Section 2 shows the antenna design and substrate details, where the design equations, substrate characteristics, as well as the evolution of the designs are shown. In section 3, the evolution of the designs is presented. Simulation and results, as well as a performance comparison with other 2.4 to 2.5 GHz resonant frequency antennas reported in the literature, with FR-4 as substrate, are shown in section 4. Finally, in section 5, some concluding remarks, and future work are given.

2. ANTENNA DESIGN

The steps followed in this research work are summarized in the flowchart shown in Fig. 1, which starts from the conception of the idea, continues with the design of the antenna, from the fundamental equations, the modifications in the geometry as part of the optimization and the simulation of the substrate requirements, until the desired results are obtained.

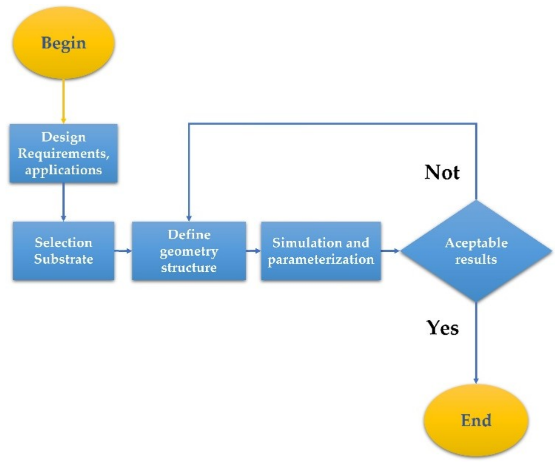

Figure 1. Flowchart of the antenna design and simulation.

It starts with a conventional rectangular microstrip-fed rectangular antenna configured at 2.4 GHz, with FR-4 as substrate. Equations [6]-[13] were used to design the antenna:

To calculate the effective dielectric constant:

$$\varepsilon_{reff}=\frac{\varepsilon_r+1}{2}+\frac{\varepsilon_r-1}{2}\left(1+12\frac{h}{w}\right)^{\frac{-1}{2}} \tag{1}$$

The increment in length (ΔL) or extent to calculate the patch length (L_p), is calculated as follows:

$$\frac{\Delta l}{h}=0.412\frac{\left(\varepsilon_{reff}+0.3\right)\left(\frac{W}{h}+0.264\right)}{\left(\varepsilon_{reff}-0.258\right)\left(\frac{W}{h}+0.8\right)} \tag{2}$$

For the calculation of the patch length, it is necessary to obtain the effective length:

$$L_p = L = L_{eff} - 2\Delta L, \quad L_{eff} = \frac{c}{f_r} = \frac{c_0}{2 f_r \sqrt{\varepsilon_{eff}}} \tag{3}$$

Finally, to calculate the patch width:

$$W_p = W = \frac{c_0}{2 f_r} \frac{(\varepsilon_r + 1)}{2}^{\frac{-1}{2}} \tag{4}$$

Equation (5) allows the calculation of the resonant frequency or center frequency of the antenna:

$$f_r = \frac{C_0}{2\left(L + 2\Delta L \sqrt{\varepsilon_{reff}}\right)} = f_c \tag{5}$$

The calculation of the dimensions of the ground plane or substrate is performed as follows: to calculate the length, the following geometric relationship was considered:

$$L_s = L + 6h \tag{6}$$

For the calculation of the substrate width, equation (7) is used:

$$W_s = W + 6h \tag{7}$$

where C_0: Free space velocity of light, f_r: Resonant frequency for the current design, ε_r: Dielectric constant of the substrate, h: Thickness of the substrate, and η: Efficiency.

The next step will be to calculate the dimensions of the microstrip (W_3 and L_3), as shown in Fig. 2b, by using the following equations [11]:

$$H = \left[\frac{Z_0 \sqrt{2(\varepsilon_r + 1)}}{119.9}\right] + \frac{1}{2}\left[\frac{\varepsilon_r - 1}{\varepsilon_r + 1}\right]\left[\ln\left(\frac{\pi}{2}\right) + \frac{1}{\varepsilon_r}\ln\left(\frac{4}{\pi}\right)\right] \tag{8}$$

$$W_f = W_1 = \left[\left(\frac{e^H}{8} - \frac{1}{4e^H}\right)^{-1}\right] \times 1.60 \times 10^{-3} \tag{9}$$

The following equations are used to calculate the dimensions, length, and width of the microstrip (L_3 and W_3) or transmission line, where the antenna feed will be coupled, as follows:

$$L_2 = L_b = \frac{\lambda}{6.25\sqrt{\varepsilon_r}}, \quad L_3 = \frac{\lambda}{4\sqrt{\varepsilon_r}}, \quad \lambda = \frac{c_0}{f_r}, \tag{10}$$

$$W_2 = W_b = \frac{\lambda}{50\sqrt{\varepsilon_r}}, \tag{11}$$

$$Z_0 = \frac{377}{\left(\left(\frac{W_3}{h} + 2\right)\left(\sqrt{\varepsilon_r}\right)\right)} \tag{12}$$

To calculate W_3, equation (12) is used, with the coupling impedance data, in this case Z_0=50 Ω.

With the above equations, the dimensions of the resonator patch located at the top of the substrate, the ground plane located at the bottom of the substrate and the dimensions of the microstrip are obtained, as shown in Fig. 2.

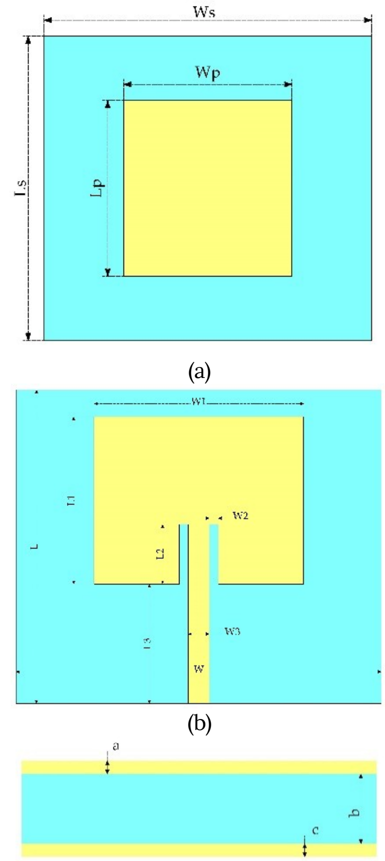

(c)

Figure 2. (a) Dimensions of the patch and substrate, (b) antenna dimensions with microstrip (initial design, with Ls=L, Ws=W, Lp=L1, and Wp=W1), c) cross-sectional view of the substrate.

The parameters used to carry out the antenna simulation are shown in Table 1. It was used FR-4 Epoxy [13], [14].

Tabla 1. Properties of FR-4.

Parameters and units	Value
Relative permittivity (ε_r)	4.4
Relative permeability	1
Dielectric Loss Tangent	0.02
Mass density	1900
Impedance port1, Z_0 (Ω)	50

Table 2 shows the dimensions of the patch antenna, the ground plane, and the dimensions of the microstrip, which were obtained with the equations described above.

Table 2. Dimensions of preliminary antenna.

Parameters	Values (mm)
Substrate length (L_s)	60
Substrate width (W_s)	60
Substrate thickness (h=b)	1.60
Patch length ($L_p = L_1$)	29.4
Patch width ($W_p = W_1$)	38
Slot length (L_2)	9.5
Slot width (W_2)	1
Microstrip width (W_3)	3
Microstrip length (L_3)	15.3

3. DESIGN SEQUENCY

3.1. Implementation of slots

The evolution of the microstrip coupled antenna is given in Fig. 2b, applying a pair of internal cuts, with dimensions calculated by equation (10) for L_2 and W_2, these cuts emulate the slots used in optics to generate constructive and destructive waves, it is implemented to observe the effect on the operating parameters of the antenna. The arrangement and location of these slots can be seen in Fig. 3.

For each slot implemented to the antenna in Fig. 3, an identifier was assigned to it, to compare the generated parameters, as shown in Table 3.

Table 3. Simulation results of antenna with slots.

Antenna	Freq (GHz)	S11 (dB)	Gain total (dB)	Bandwidth (MHz)	VSWR <2	Efficiency (η)
Initial Design	2.22	-22.81	2.22	118.8	1.25	0.085
Slots 1	2.23	-24.49	2.14	56.3	1.03	0.44
Slots 2	2.20	-20.85	1.55	55.5	1.57	0.38
Slots 3	2.18	-21.27	1.71	57.3	1.5	0.43
Slots 4	2.19	-24.77	1.58	54.8	1	0.41

The responses shown by the four designs allow selecting only one of these, since the combination of two or more slots in the antenna impacts negatively decreasing the gain, the efficiency and the center frequency is moving away from the target (2.4 GHz). Therefore, the antenna slots 1 is chosen to continue with the next step.

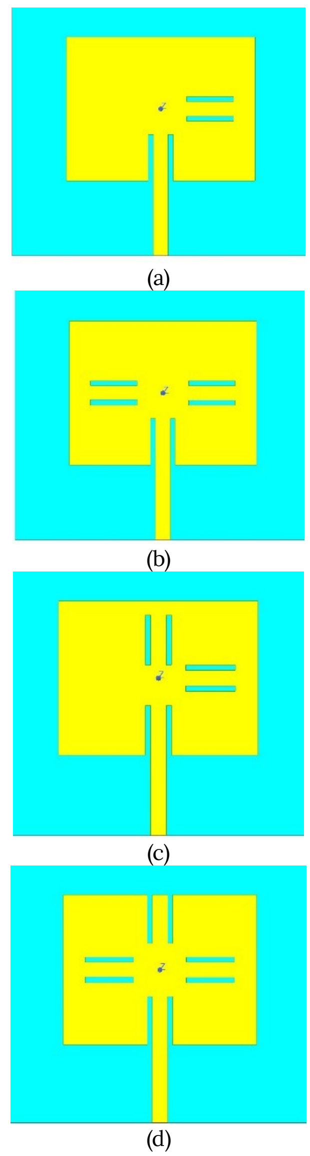

Figure 3. Patch antenna named (a) Slots 1, (b) Slots 2, (c) Slots 3 and (d) Slots 4.

3.2. Implementation of antenna corner cuts

On the design, slots 1, some geometrical optimizations will be developed, starting with four cuts at the corners of the patch applying the following geometrical relations described in Fig. 4a and 4b:

Length of the corner cuts	Equation	
2.5 mm	$L_a = W_a = \frac{\lambda}{(24\sqrt{\varepsilon_r})}$	(13)
3 mm	$L_a = W_a = \frac{\lambda}{(20\sqrt{\varepsilon_r})}$	(14)
3.5 mm	$L_a = W_a = \frac{\lambda}{(17\sqrt{\varepsilon_r})}$	(15)
4.5 mm	$L_a = W_a = W_4 = \frac{\lambda}{(13\sqrt{\varepsilon_r})}$	(16)
5 mm	$L_a = W_a = \frac{\lambda}{(12\sqrt{\varepsilon_r})}$	(17)
5.45 mm	$L_a = W_a = \frac{\lambda}{(10.9\sqrt{\varepsilon_r})}$	(18)
5.5 mm	$L_a = W_a = \frac{\lambda}{(10.75\sqrt{\varepsilon_r})}$	(19)
5.6 mm	$L_a = W_a = \frac{\lambda}{(10.65\sqrt{\varepsilon_r})}$	(20)
5.75 mm	$L_a = W_a = \frac{\lambda}{(10.35\sqrt{\varepsilon_r})}$	(21)
6 mm	$L_a = W_a = \frac{\lambda}{(10\sqrt{\varepsilon_r})}$	(22)
6.5 mm	$L_a = W_a = \frac{\lambda}{(9.2\sqrt{\varepsilon_r})}$	(23)

The slots separation was obtained from:

$$d_1 = \frac{\lambda}{15\sqrt{\varepsilon_r}} \qquad (24)$$

These are equations for the geometrical relationships of the corner cuts and provided the best response within the center frequencies of the 2.4 GHz antenna. Fig. 4 shows the dimensions for the corresponding corner cuts and slots.

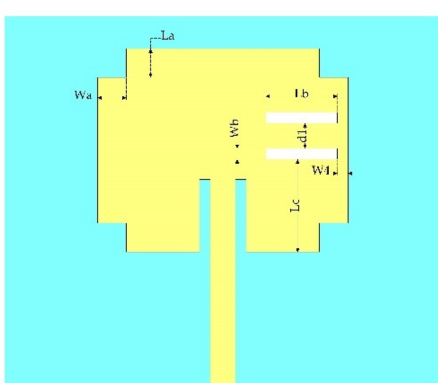

Figure. 4. Dimensioning for the parameterization of the corner cuts.

Geometric optimization was applied to the corners of the antenna by applying cuts from 2.5 mm to 6.5 mm as shown in equations (13 to 24). These cuts generated the resonant frequency behaviors with respect to the reflection coefficient S11, the standing wave ratio VSWR and gain, shown in Fig. 5.

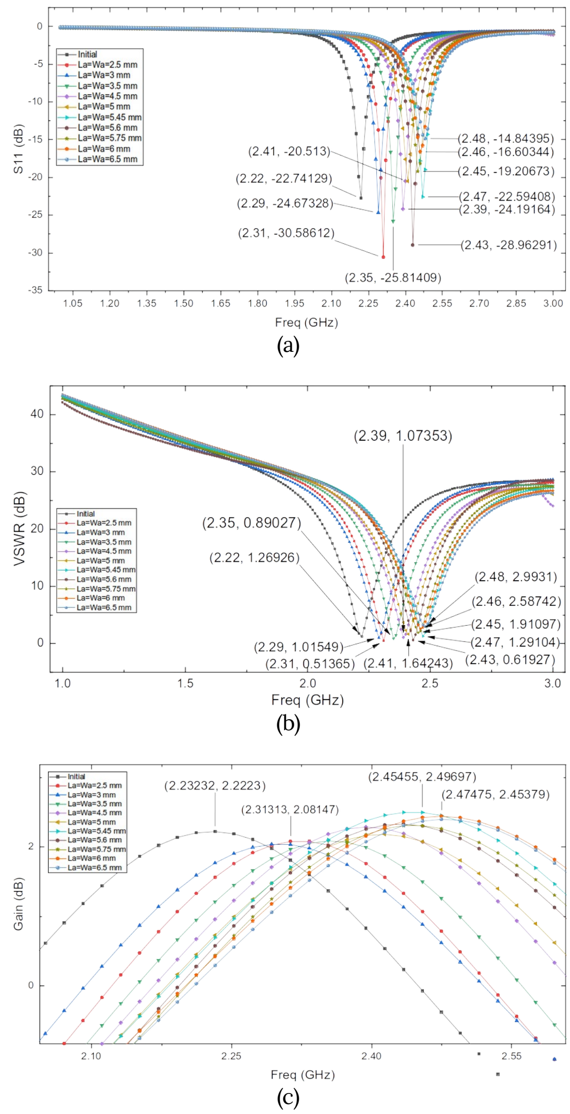

Figure 5. Behavior of (a) frequency vs S11, (b) frequency vs VSWR and (c) frequency vs Gain of all the corner cuts performed on the antenna.

Based on the graphical behavior of the antenna parameters, Table 4 is generated, where the results generated by the corner cuts are summarized. The corner cuts were performed symmetrically so that the length and width were varied in the same conditions and dimensions.

From Table 4, it is observed that the device with the corner cut at 5.6 mm has the best VSWR response (0.61), this is an acceptable value result in accordance with [7]. In addition, it has an operating frequency of 2.43 GHz with S11=-28.96 dB, values adequate for biomedical applications [13],[14].

Table 4. Antenna results when corner cuts were applied.

Design or corner cots length (mm)	f_c=f_r (GHz)	S11 (dB)	VSWR <2	Gain (dB)	BW (MHz)	η
Fig 2b	2.22	-22.81	1.25	2.22	60.5	0.45 and 0.085 in 2.4 GHz
Fig 3a	2.23	-24.49	1.03	2.14	56.3	0.44 and 0.0748 in 2.4 GHz
2.5	2.31	-30.58	0.51	2.08	60.7	0.43 and 0.18 in 2.4 GHz
3	2.29	-24.67	1.01	2.03	64.6	0.35 and 0.2798 in 2.4 GHz
3.5	2.35	-25.81	0.89	2.08	60.2	0.42 and 0.27 in 2.4 GHz
4.5	2.39	-24.19	1.07	2.28	62.2	0.447 and 0.444 in 2.4 GHz
5	2.41	-20.51	1.64	2.18	67.5	0.44
5.45	2.47	-22.59	1.29	2.49	69.8	0.46
5.6	2.43	-28.96	0.61	2.33	66	0.44
5.75	2.45	-19.20	1.91	2.3	66.9	0.44
6	2.46	-16.60	2.58	2.39	69	0.43
6.5	2.48	-15.35	2.99	2.39	63.2	0.42

3.3. Implementation of a top notch

The design of the antenna with the corner cuts of 5.6 mm was chosen to continue optimizing the antenna. Now, a symmetrical notch will be made on the edge or top side of the patch with respect to the microstrip, see Fig. 6.

Initially, the notch is applied with the following dimensions W_b=1 mm and L_b=L_2=9.5 mm. Subsequently, the optimization will be performed by increasing W_b by 1, 3, 5, 5, 6 and 6.5 mm, since these are the dimensions that generated results within the resonance frequency. The parameterization is performed without moving to L_2=9.5 mm, as shown in Table 5.

This result allows selecting the notch width W_b=6 mm, since the gain is higher with respect to the design without top notch in Table 4. In addition, the VSWR<2 and S11 is still in acceptable parameter (< -10 dB).

Table 5. Results when applying a different Wb.

Notch width W_b (mm) with L_b=9.5	f_c=f_r (GHz)	S11 (dB)	VSWR <2	Gain (dB)	BW (MHz)	η
$W_b=\frac{\lambda}{(50\sqrt{\varepsilon_r})}=1$	2.44	-18	2.19	2.27	63.2	0.41
$W_b=\frac{\lambda}{(20\sqrt{\varepsilon_r})}=3$	2.45	-19.9	1.76	2.43	67.3	0.44
$W_b=\frac{\lambda}{(12\sqrt{\varepsilon_r})}=5$	2.46	-20.8	1.59	2.30	64.7	0.45
$W_b=\frac{\lambda}{(10\sqrt{\varepsilon_r})}=6$	2.48	-20.9	1.55	2.47	64.4	0.42
$W_b=\frac{\lambda}{(9.2\sqrt{\varepsilon_r})}=6.5$	2.49	-18	1.99	2.17	63.1	0.39

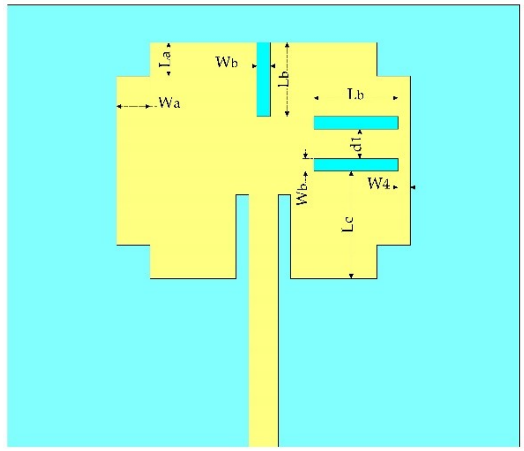

(a)

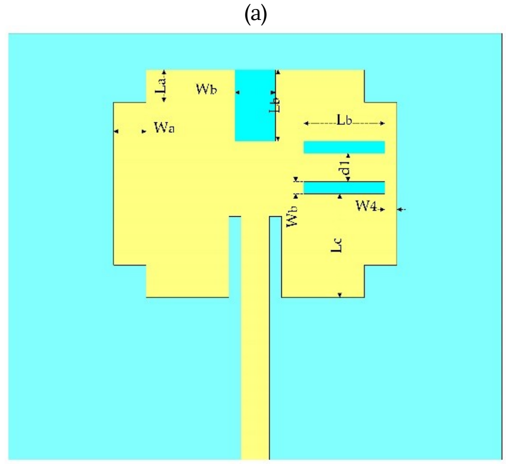

(b)

Figure 6. Optimization of the antenna with microstrip applying corner cuts and a top notch (a) initial design, and (b) final design

By selecting to W_b=6 mm, the next step in the optimization is to make a dimension variation in the notch now considering its length dimension L_b. For this parameterization the first six dimensional variations were placed that generate results within the resonant frequency bandwidth, these results can be observed in Table 6.

The final notch dimensions are L_b=6 mm and W_b =6 mm, since, as shown in Table 6, it is the one that provides the best response in the antenna operating parameters.

Table 6. Results when applying a top notch on the antenna with different L_b.

Length of notch, with with W_b=6 (mm)	f_c=f_r (GHz)	S11 (dB)	VSWR <2	Gain (dB)	BW (MHz)	η
$L_b=\frac{\lambda}{(8.5\sqrt{\varepsilon_r})}=7$	2.5	-18.93	2	2.61	67.4	0.43
$L_b=\frac{\lambda}{(9.2\sqrt{\varepsilon_r})}=6.5$	2.49	-22.12	1.36	2.58	66.6	0.43
$L_b=\frac{\lambda}{(10\sqrt{\varepsilon_r})}=6$	2.5	-22.16	1.35	2.96	69	0.47
$L_b=\frac{\lambda}{(12\sqrt{\varepsilon_r})}=5$	2.49	-18.36	2.1	2.56	67.2	0.43
$L_b=\frac{\lambda}{(13\sqrt{\varepsilon_r})}=4.5$	2.51	-20.49	1.64	2.73	70.5	0.44
$L_b=\frac{\lambda}{(15\sqrt{\varepsilon_r})}=4$	2.47	-18.17	2.13	2.67	66.9	0.44

4. SIMULATION RESULTS

Table 7 summarizes the results of the last optimized designs with the fundamental operating parameters of the microstrip patch antenna.

Table 7. Results of the antennas that obtained acceptable parameter values.

ID	Antenna	Freq (GHz)	S11 (dB)	Gain total (dB)	Bandwidth (MHz)	VSWR <2	η
Design 1	Initial design	2.22	-22.81	2.22	118.8	1.25	0.085
Design 2	Slot 1	2.23	-24.49	2.14	56.3	1.03	0.44
Design 3	W_a=L_a= 5.6 mm	2.43	-28.96	2.33	66	0.61	0.44
Design 4	$W_b=\frac{\lambda}{(10\sqrt{\varepsilon_r})}=6mm$ L_b =9.5mm	2.48	-20.9	2.47	64.4	1.55	0.42
Final Design	$L_b=\frac{\lambda}{(10\sqrt{\varepsilon_r})}=6mm$ L_b= 6 mm	2.5	-22.16	2.96	69	1.35	0.47

Thus, as can be seen, the evolution of the optimization allows the generation of an antenna for each applied element:

- Antenna with 1 mm x 9.5 mm slots (design 2).
- Antenna with the slots and 5.6 mm x 5.6 mm corner cuts (design 3).
- Antenna with 1 mm x 9.5 mm slot, 5.6 mm x 5.6 mm corner cuts and 6 mm x 9.5 mm top notch (design 4).
- Antenna with 1 mm x 9.5 mm slot, 5.6 mm x 5.6 mm corner cuts and top notch of 6 mm x 6 mm (final design, Fig. 6b).

On the other hand, to observe the graphical behaviors of the gain, S11, VSWR and efficiency (η) parameters with respect to a frequency sweep of the five designs shown in Table 7, the operating curves of the five designs from the preliminary antenna to the last optimized design are given, in Fig. 7.

The comparison of the final antenna design with other ones reported in literature is given in Table 8.

Table 8. Comparison of our antenna design with other antennas reported.

Ref	Freq (GHz)	S11 (dB)	VSWR	Gain (dB)	Bandwidth (MHz)	Size patch (mm)	Total substrate (mm)
[10]	2.41	-14.10	1.49	2.65	53.6	25x25	FR-4, 50x50x1.6
[11]	2.40	-15.28	---	3.05	---	30x37	FR-4
[12]	2.40	-22.21	---	1.6	70	29x28	FR-4, 60x66.2x1.6
[13]	2.40	-31	---	---	---	38.02x28 .78	FR-4, 56x56x1.6
This work	2.5	-22.16	1.35	2.96	69	See Table 2	

According to the results obtained, we see that our optimized antenna has acceptable response, since it has the most negative values of S11, it is competitive in gain with [11][and in bandwidth with [12]. It should be noted that in this work we developed exclusively the geometric or structural parameterization technique, where modifications were applied in dimensions, without connecting or attaching additional elements, such as films or using metamaterials that doped the resonator element, which some authors apply to obtain better responses [2], [7].

5. CONCLUSIONS

It is shown that, from the implementation of slots, the application of corner cuts and the geometrical parameterization for the determination of the notch dimensions, allow to optimize the antenna design. The equations of the geometrical relationships that allowed the parameterization of the dimensions in the antenna corner cuts and top notch are also provided.

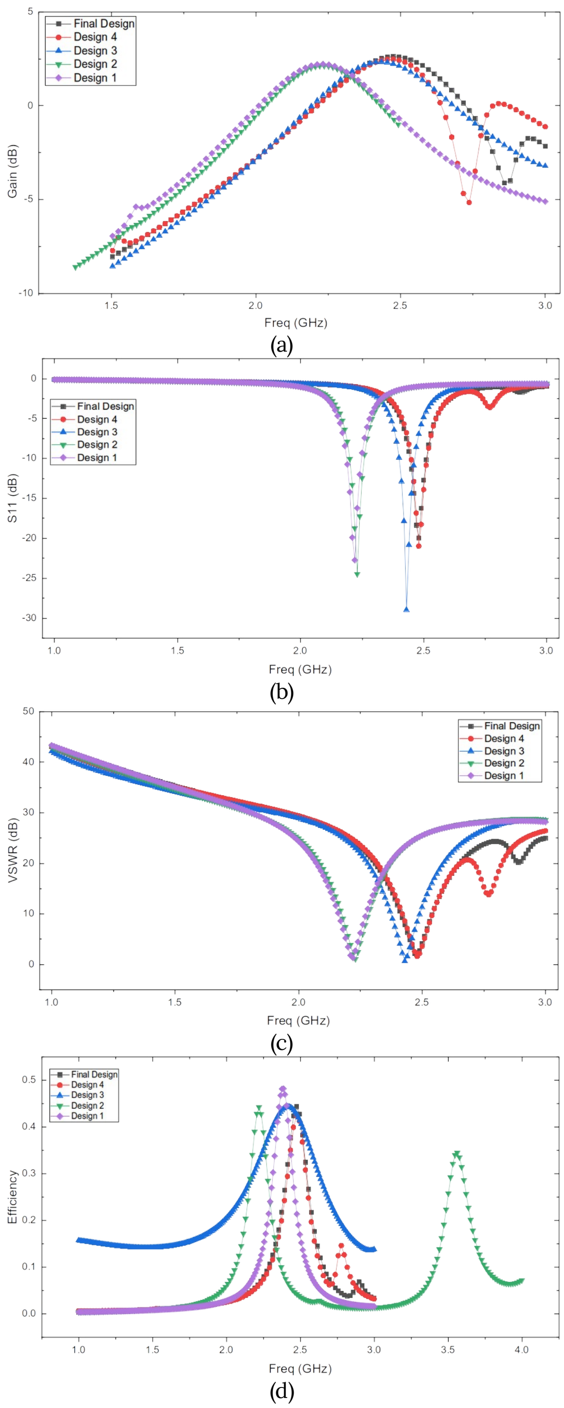

Figure 7. (a) Gain, (b) S11, (c) VSWR, and (d) efficiency, when a frequency sweep is applied.

The percentage increase in gain with respect to the initial antenna is 34.54%, and the efficiency increased by 552.94%. The optimized antenna has operation frequency at 2.5 GHz. It is known that, due to the manufacturing process and materials used, the center frequency will have a slight shift to the left. Then, in practice, the operation frequency would be located very near to 2.45 GHz, which is the operation frequency considered in Table 9. In case, it would be possible to make the necessary adjustments.

Future work

The next stage with the optimization shown here and the data of the permittivity and conductivity of the tissues (shown in Table 9) will allow these antennas to be simulated to consider their effects on such tissues.

Table 9. Dielectric properties of human tissues at 2.45 GHz [1-3].

Ref	Freq (GHz)	S11 (dB)
Tissues	Relative permittivity (ε_r)	Conductivity (S/m)
Muscle	52.7	1.73
skin	38	1.46
Fat	5.28	0.10
Bone	18.54	0.80

Subsequently, fabrication and laboratory tests will be carried out with materials that emulate the tissues, to validate the corresponding responses. To carry out the laboratory tests and emulate these tissues, the data in Table 10 will be used as a reference.

Table 10. Preparation about phantom liquids [1-3,14].

Ingredients	Skin	Fat
Deionized water	50%	2.9%
NaCl	-	0.1%
Sugar	50%	-
Vegetable oil	-	30 %
Flour	-	67 %

Acknowledgements

Pedro Vargas-Chable is grateful to CONAHCYT for his postdoctoral stay (CVU 484392). M. Tecpoyotl-Torres for SNI support (CVU 20650).

REFERENCES

[1] Ashok Kumar, S., T. Shanmuganantham. Design of Clover Slot Antenna for Biomedical Applications. *Alexandria Engineering Journal*. 2017, 56(3), 313–317. doi:.10.1016/j.aej.2016.08.034.

[2] Mahalakshmi, N., A. Thenmozhi. Design of Hexagon Shape Bow-Tie Patch Antenna for Implantable Bio-

Medical Applications. *Alexandria Engineering Journal*. 2017, 56(2), 235–239. doi: 10.1016/j.aej.2017.01.028.

[3] Soontornpipit, P A Dual-Band Compact Microstrip Patch Antenna for 403.5 MHz and 2.45 GHz on-Body Communications. *Procedia Computer Science*. 2016, 232–235. doi: 10.1016/j.procs.2016.05.105.

[4] Ortega-Palacios, R., Trujillo-Romero, C. J., Cepeda Rubio, M. F., Vera, A., Leija, L., Reyes, J.L., Ramírez-Estudillo, M. C., Morales-Alvarez, F., Vega-López, M. A. Feasibility of Using a Novel 2.45 GHz Double Short Distance Slot Coaxial Antenna for Minimally Invasive Cancer Breast Microwave Ablation Therapy: Computational Model, Phantom, and in Vivo Swine Experimentation. *Journal of Healthcare Engineering*. 2018, 1–10. doi: 10.1155/2018/5806753.

[5] Liu, L., Peng, A., Xiaonan,W., Chaoqun, Z. Measurement Analysis of Polarization Distribution of Static On-Body Propagation Channels. In: 7th IEEE *International Symposium on Microwave, Antenna, Propagation, and EMC Technologies* (MAPE). 2017. doi:10.1109/mape.2017.8250787.

[6] Younes, S., Kaoutar, S. A., Jaouad, F. Study and Design of a Patch Antenna for Biomedical Applications. In: *ITM Web of Conferences*. 2023, 03003. doi: 10.1051/itmconf/20235203003.

[7] Sarmah, K., Angan, S., Kandarpa, K. S., Sunandan, B. Dual-Band Microstrip Patch Antenna Loaded with Complementary Split Ring Resonator for WLAN Applications. *Advances in Intelligent Systems and Computing*. 2015, 573–80. doi: 10.1007/978-81-322-2250-7_57.

[8] Khraisat, Y. S. Increasing Microstrip Patch Antenna Bandwidth by Inserting Ground Slots. *Journal of Electromagnetic Analysis and Applications*. 2018, 10(1), 1–11. doi: 10.4236/jemaa.2018.101001.

[9] Siju, J. T., Mehajabeen, F. Bandwidth Improvement of Microstrip Patch Antenna Using Partial Ground Plane. *International Journal of Engineering Research*. 2015, 4(5). doi: 10.17577/ijertv4is050205.

[10] Küçükcan, S., Kaya, A. Dual-band Microstrip patch antenna design for Wi-Fi Applications. *European Journal of Science and Technology*. 2022. doi: 10.31590/ejosat.1084147.

[11] Mohd-Zaini, S. R., Abdul-Rani, K. N. Wearable inset-fed FR4 microstrip patch antenna design. In: *IOP Conference Series: Materials Science and Engineering*. 2018, 318, 012050. Available from: doi:10.1088/1757-899x/318/1/012050.

[12] Adnan, M. A., Kamilia, K., Yamada, Y., Idris, I. H., Ali, A. A., Hamdan, H. Biocompatible sago aerogel material as a substrate for antenna application. *Journal of Physics: Conference Series*. 2022, 2250(1), 012005. doi: 10.1088/1742-6596/2250/1/012005.

[13] Singh, J., Singh, T., Sohi, B. S. Design of slit loaded rectangular microstrip patch antenna. In: 2nd *International Conference on Recent Advances in Engineering & Computational Sciences*. 2015. doi: 10.1109/raecs.2015.7453359

[14] Sukhija, S., Sarin, R. K. Design and performance of two-sleeve low profile antenna for bio-medical applications. *Journal of Electrical Systems and Information Technology*. 2017, 4(1), 49–61. doi: 10.1016/j.jesit.2016.10.013.

ABOUT THE AUTHORS

Pedro Vargas Chable obtained a B.S. degree in Electrical and Electronics Engineering from the Universidad Juarez Autonoma de Tabasco in 2008. From 2009 to 2012 he worked as a Specialist in the Evaluations of Lighting Conditions and Non-Ionizing Radiation under NOM-025 and 013 of the STPS respectively, as well as signatory before the ema of the latter in the company Tecnología del Ambiente S. A de C. V. From 2012 and 2019 he obtained the degree of Master and PhD in Engineering and Applied Sciences with Terminal option in Electrical Technology, by the Autonomous University of the State of Morelos (UAEM). In October 2023, he became a member of the Sociedad Mexicana de Materiales A. C. He is currently working on the development of antennas for biomedical applications, design, simulation, and modeling of microactuators, microgripper, accelerometers, RF MEMS and VLSI devices applying Finite Element Analysis (FEA).

Margarita Tecpoyotl Torres received the Mathematician degree from the University of Puebla, Mexico (1991). She was also graduated as Electronic Engineer (1993). She received the M.Sc. and Ph.D. degrees in Electronics from National Institute of Astrophysics, Optics and Electronics, INAOE, México (1997 and 1999, respectively). Dr. Tecpoyotl works, since 1999, at UAEM, Mexico, where she is currently titular professor. She has been visiting research scientist at University of Bristol (2001), UK. She led the Winner team of Boot Camp, UAEM Potential, obtaining support to participate in Full Immersion Program, USA

(2014). She won the 3rd place in the Royal Academy of Engineering´s Leaders in Innovation Fellowships final pitch session, in UK (2015). Her main research interest includes MEMS, Antenna design, entrepreneurship, innovation, and development of educational programs. She holds the status of National Researcher (SNI), since 1999.

Ramon Cabello Ruíz received the Engineer Mechanical degree from the Autonomous University of the State of Morelos, Mexico (2010). He received the M. Eng. And Ph.D. degrees in Center for Research in Engineering and Applied Sciences, Mexico (2012 and 2017, respectively). He holds three SolidWorks certifications, (Mechanical Design level Associate, Mechanical Design level Professional, and Simulation level Associate). Dr. Cabello Works, since 2019, at UAEM, Mexico, where he is a part-time teacher. His area of expertise focuses on the design and mechanical analysis of microelectromechanical systems. He holds the status of National Researcher (SNI), since 2023. He is also a member of the National Register of Researchers in Materials Sciences.

Dr. Mireles Jr. is currently a Research Professor of the Department of Electrical and Computer Engineering of the Institute of Engineering and Technology of UACJ since July 1996. He is an External Member of the Graduate School of Engineering of the University of Texas in El Paso (UTEP) since 2016. Graduated from the University of Texas at Arlington (Ph.D.) in 2002, and from the Instituto Tecnologico de Chihuahua, (M.Sc.) in 1996. Head and founder of CICTA from UACJ where he has developed several Technological Development and Innovation projects with patents in Microtechnology. He has been director and co-director of national network projects, and technical director during the establishment of innovation centers in the state of Chihuahua, such as: CICTA, the Center for Molds and Dies of the State of Chihuahua (CIMIT), and the IA Center in which he currently serves as liaison director of projects development.